ExoPlanet Optics: conceptual design processes for stealth telescopes

J. B. Breckinridge, J. E. Harvey, R. Irvin, R. Chipman, M. Kupinski, et al.

J. B. Breckinridge, J. E. Harvey, R. Irvin, R. Chipman, M. Kupinski, J. Davis, D-W. Kim, E. Douglas, C. F. Lillie, T. Hull, "ExoPlanet Optics: conceptual design processes for stealth telescopes," Proc. SPIE 11115, UV/Optical/IR Space Telescopes and Instruments: Innovative Technologies and Concepts IX, 111150H (9 September 2019); doi: 10.1117/12.2528825

SPIE.

Event: SPIE Optical Engineering + Applications, 2019, San Diego, California, United States

ExoPlanet Optics: conceptual design processes for stealth telescopes

J. B. Breckinridge*[a,b], J. E. Harvey[c], R. Irvin[c], R. Chipman[b], M. Kupinski[b], J. Davis[b], D-W Kim[b], E. Douglas[d], C. F. Lillie[e], T. Hull[f]

[a]Galcit, California Institute of Technology, 1200 California Blvd., Pasadena, CA 91125; [b]College of Optical Sciences, University of AZ, Tucson, AZ. 85711; [c]Photon Engineering, 310 S Williams Blvd #222, Tucson, AZ 85711, [d]Steward Observatory, University of Arizona, Tucson AZ 85721; [e]Lillie Consulting, LLC, 6202 Vista del Mar, Playa del Rey, CA, USA 90293, and [f]University of New Mexico, Albuquerque, NM.

ABSTRACT

In this paper we examine several contrast-degrading static signature sources present in current terrestrial exoplanet Lyot Coronagraph/Telescope optical systems. These are:

- Unnecessary optical surfaces, which increase cost, absorption, scatter, wavefront control and alignment issues. A suggested solution is to make every effort to investigate innovative solutions to reduce the number of optical surfaces during the early design phase. Consider free-form optics.
- Diffraction from secondary support systems and classical hexagon segmented apertures, which masks the low IWA terrestrial exoplanets. A suggested mitigation is to investigate curved secondary support systems and a pinwheel architecture for the deployable primary aperture.
- Polarization Fresnel and form birefringence aberrations, which distort the system PSF, introduce absorption, scatter and wavefront control issues. Mitigation is to reduce all ray-angles of incidence to a minimum, investigate zero-loss polarization compensation wavefront technology, and investigate metal thin film deposition processes required to minimize form birefringence in large-area high-reflectivity coatings.
- Small-angle specular or resolved angle scattered light, which places a narrow halo of incoherent light around the base of the PSF. There is no requirement on mirror smooth-surface scatter. Investigate the physical source of the small angle scatter & develop mirror polishing & thin film deposition processes to minimize scatter.

Keywords: Terrestrial exoplanet imaging, HabEx, LUVOIR, space telescopes, coronagraphs, optical design, polarization, diffraction, mirror surface scatter

----- ----- ----- -----

Further author information: send correspondence to J. B. Breckinridge: email: jbreckin@caltech.edu

1. INTRODUCTION

Optical systems for the characterization of terrestrial exoplanets are, without a doubt the most challenging optical engineering development this century. The requirement is to extract optical spectra, at spectral resolutions, $[\lambda/\delta\lambda] > 50$, from a terrestrial exoplanet a few Airy diffraction rings from a star that is ten billion (10^{10}) times brighter than the exoplanet. On first glance this seems impossible. But scientists and engineers have almost achieved this optical performance routinely in the laboratory today. It remains, however to successfully transition this technology from the laboratory to a reliable and affordable space flight optical instrument, capable of years of operation in deep space, far from the earth.

All optical systems imprint their signature on recorded images. Some of these signatures mask important scientific information. An ideal telescope/instrument system would emulate a perfectly open clear aperture with zero scattered light, zero geometric aberrations, 100% transmittance and zero polarization with perfect optical filters and/or dispersive elements. Diffraction and it's apodization are the only limiting factor that we have no control over. We call such an optical system "stealth" because it imparts the minimum signature onto the data as though the telescope/instrument were not present. Such an optical system will maximize the quality of the science data and simplify the calibration to restore accurate source irradiance. A "stealthy" telescope is required to image and characterize terrestrial exoplanets.

UV/Optical/IR Space Telescopes and Instruments: Innovative Technologies and Concepts IX, edited by Allison A. Barto, James B. Breckinridge, H. Philip Stahl, Proc. of SPIE Vol. 11115, 111150H · © 2019 SPIE
CCC code: 0277-786X/19/$21 · doi: 10.1117/12.2528825

2. COST, SCHEDULE & PERFORMANCE

Many years of experience building successful instruments for space science has shown that the concept design phase is, perhaps the most important phase of development.[1] It is here that the implementation direction and thus cost and performance are established. It is useful to report a few rules to remember during the concept development phase for space optical instruments. 1. **Form follows function**, that is the design team must keep in mind the function of the optical system in flight. Adding functions that are not aligned to the primary goal of the instrument increases cost and complexity and distracts from the engineering process. **2. KISS (Keep It Simple for Space)**. Remember access to space to repair broken complicated subsystems is extremely expensive. And hardening a complicated system design for space flight is EXTREMELY expensive and failure risk is high. Find a robust design concept that is cost effective to build, maintain and perhaps "self-healing". **3. Understand requirements.** All members of the development team need to be intimately familiar with the requirements and understand fully how subsystems interact with each other to create the high-performance instrument. **4. Respect experience.** Listen, understand and respect clever innovative solutions suggested by others. **5. Remain objective, because people who say:**

- "I invented this instrument, I own the design, dollars are invested already and I'll force it to work at all cost" . . . . Often leads to failure!
- "My space-science proposal was awarded to me to build my specific space instrument I designed and only I can build it" . . . . . Often leads to failure!
- "Everyone else does it this way it must always be right" . . . .Not always!

Cost schedule & performance (c,s,p) are the three axes that a task or project moves within. These three coordinate axes define the volume that constrains the development of space telescopes and instruments. Figure 1. shows this three-dimensional volume. The project or task at a fixed time is identified by a point in the volume. As time passes the point moves inside the volume. These three axes are not orthogonal, that is they are not independent. For example, increasing schedule almost never reduces cost. During the design concept phase all ideas to improve performance by adding features or subsystems must be thought of in terms of the drawing in Figure 1. Sometimes innovation may lead to reduced cost or increase performance, as we shall see later in this paper. However, the earlier in the project these innovations are applied, the lower the final cost.

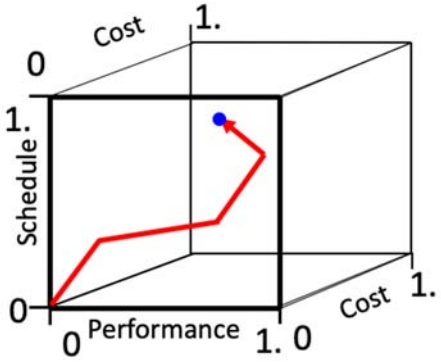

Figure 1. Projects and tasks move within the boundaries of cost, schedule and performance.

3. LYOT CORONAGRAPH FOR TERRESTRIAL EXOPLANETS

Breckinridge (1984)[2] first suggested that space telescopes to directly image and characterize exoplanets are feasible and provided a design concept for an optical system. The past 34 years have seen many advances in exoplanet science and measurement technology. An optical system design approach to minimize telescope/instrument system signatures is essential to make successful measurements of terrestrial exoplanets and will be used here as an example.

One of the optical layouts most likely to be successful in direct imaging terrestrial exoplanets is the Lyot Coronagraph, originally conceived by Bernard Lyot.[3] Success is measured by the ability of the instrument to measure spectra from the exoplanet surface, its atmosphere and surrounding gas and dust. Fig 2 below shows a schematic of the layout for the classical Lyot coronagraph. In this paper we examine first order conceptual designs in order to explore design opportunities & constraints.

Additional surfaces are added to the optical system shown in Fig 2 to control wavefront errors introduced by surface fabrication errors and by dynamic wavefront errors introduced by pointing, structural and thermal time-dependent errors. However, the basic system function, represented in Fig 2 by the minimum number of surfaces remains unchanged.

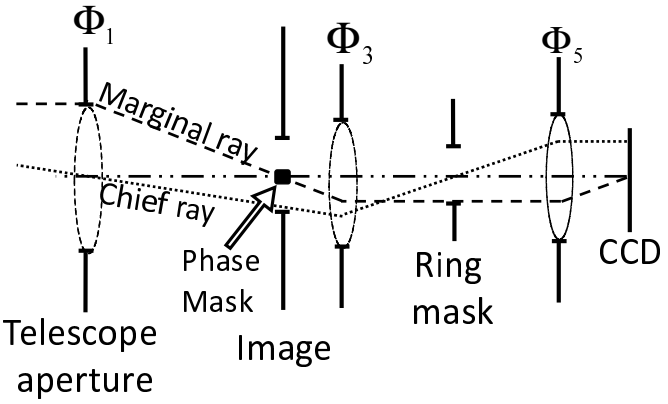

Fig. 2 Shows a schematic of a Lyot Coronagraph giving the minimum number of optical elements required to perform a needed function. Light enters from the left and strikes the entrance aperture at plane 1 which has optical power Φ_1. The marginal ray crosses the axis at the image plane where we locate an amplitude and phase mask. The field-of-view in the exoplanet coronagraph is very small and the chief ray angle at the entrance aperture is typically less than 30 arc-seconds. An optical element with power Φ_3 is located to the right of the image plane. This optical element is positioned to perform two functions: it collimates light from the image plane and relays an image of the complex field at the telescope aperture onto a surface where we position a ring-mask. This ring mask, often called the Lyot stop is sized to block light that diffracts around the edge of the entrance aperture (at surface 1). This effectively makes the aperture of the telescope smaller, but by blocking diffracted light that scatters around this aperture edge the amount of light transmitted further into the system is reduced, thus increasing coronagraph contrast. A relay optic at surface 5 which has optical power Φ_5 relays the image onto the final image plane where the complex electric field is converted to intensity at the detector (CCD).

4. TELESCOPE/INSTRUMENT SIGNATURES

All telescope/instrument systems imprint their unique signatures onto the image which may mask important scientific information. Minimizing this signature will maximize the scientific usefulness of the telescope/instrument system and in this case will enable direct imaging and spectroscopy of terrestrial exoplanet surfaces and atmospheres.

Dynamic signature sources are those which arise from events that cause time-dependent changes to the end-to-end optical system performance during the long integration times necessary to record signals from the very faint exoplanets. Examples are spacecraft vibration, pointing & control, thermal expansion, contraction of the structure and time-changing optical contamination & radiation damage. Dynamic signatures are examined in detail elsewhere[4].

Static signature sources include absorption of light by mirrors, lenses & filters and diffraction of light by segments & secondary support structure & the edge of the entrance aperture and polarization aberrations and geometric aberrations and scattered light (specular and small angle). In this paper we will examine four static signature sources: 1. unnecessary optical surfaces, 2. scalar diffraction, 3. polarization aberration, and 4. small angle specular scattered light.

5. UNECESSARY OPTICAL SURFACES ARE BAD

C. F. Lillie and J. B. Breckinridge[5] show that for 10-meter class telescopes the cost impact of adding one additional optical surface is between 100 and 500 million dollars. This calculation includes the cost to increase the aperture to compensate for absorption loss and the cost to fabricate the optical surface and the cost to hold the optic to the needed tolerance and the labor to manufacture, and integrate the surface.

Adding one additional optical surface means that the tolerances (surface figure & mechanical support & stability) on all of the other surfaces need to increase and the tolerance becomes more difficult to achieve and thus more expensive. Consider the example of a diffraction-limited system with 4 surfaces where the rms geometric wavefront error is the same on each of the 4, say 4.5 nm. Then if a 5th mirror is then added to the system, the allowable rms geometric wavefront error on the surfaces and the mechanical stability in terms of tip, tilt and piston of each of these 5 mirrors is decreased by 12%. Opto-mechanical tolerances have become tighter and more expensive, if achievable. In addition, the system transmittance is decreased from 0.97^4 to 0.97^5 and the aperture size needs to be increased to compensate for loss in the SNR. All of this adds cost and schedule to the program in order to retain the required system requirement.

Adaptive optics (A/O) are used to correct for wavefront errors between zero and about 100 cycles per beam diameter. However, 2 or 3 additional reflections, each with their own inherent absorption losses are needed to implement A/O. This correction method is effective at the expense of system transmittance, cost and complexity/risk. An alternative is to develop A/O technology that allows the use of curved active mirrors. A/O recovers some alignment tolerance issues, but is not able to:

Recover lost optical power in the system
Completely correct for polarization aberrations[6] and
Correct mirror-surface narrow-angle scattered light[7].

A/O is an essential part of exoplanet coronagraph systems and the highest contrast cannot be obtained without it. However, the optical system design concept that employs them must be well thought out to maximize performance, avoid excessive absorption and minimize risk during flight.

Optical surfaces that perform multiple functions, such as placing a diffraction grating on an aspheric surface is an example of a design approach to reduce the number of surfaces. Implementing this approach provides both wavefront control and dispersion for spectroscopy, with reduced opto-mechanical complexity and decreased risk. The new technology of free-form optics[8] will enable improved designs for low cost high efficiency and should be considered during the concept design phase.

6. DIFFRACTION

In this section, we recognize that the telescope/coronagraph complex-wave optical system performance needs to be optimized end-to-end. That is, the complex-wave performance of the telescope must be designed to match that of the coronagraph system if we expect the end-to-end optical performance to be optimum for exoplanet characterization. The two optical systems need to be pair-wise optimized during both the design approach phase and later at the detailed design phase.

Large aperture telescope systems are segmented for manufacturing, assembly and packaging for launch purposes. Today, these segments project unique signatures across the image plane. Large aperture telescope primary mirrors are partitioned into arrays of hexagonally shaped segments. For structural purposes and to enable in-space deployment there are gaps between these segments. These periodic gaps diffract light across the image plane which mask exoplanets and pollute the faint exoplanet spectra with light from the parent star. The periodic structure topology used today across large primary apertures causes unwanted ghost images of the star which may mask exoplanets.

Figure 3 left, given below shows the aperture for a “typical” classic segmented telescope, tessellated using regular hexagonal segments. The figure on the right shows the image plane monochromatic irradiance for the aperture on the left. Looking at the aperture to the left we see that the gap-lines that separate the segments line-up to form segments of slits and we see that these “broken” slits form an array of slits whose spacing we identify as w/2 where w is the face-to-face width of each regular mirror segment. The hexagonal symmetry of the segments results in the hexagonal symmetry shown in the PSF at the right in this figure. The irradiance distribution at the image plane of a 10-meter segmented aperture is shown at the right covering the center 1 x 1 arc second field of view.

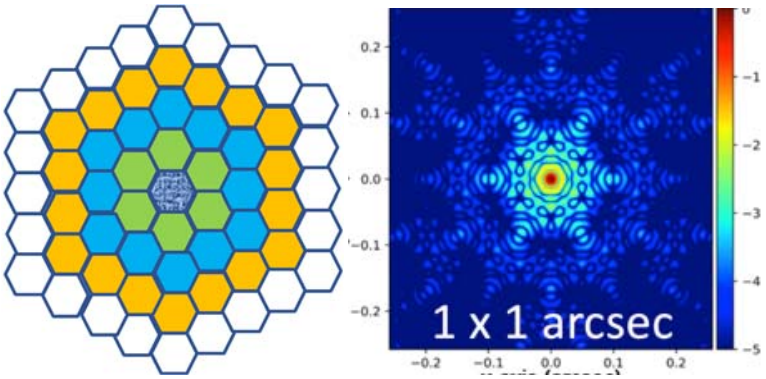

Figure 3 Left: classic segmented telescope 10-m class aperture tessellated using hexagonal segments. Right: corresponding complicated point spread function (PSF) or signature characteristic of the aperture segmentation pattern shown to the left. The PSF brightness scale is Log_{10}.

We want to characterize terrestrial exoplanets in the habitable zone to maximize our probability of finding life like ours. Therefore, it is of interest to calculate the location of earth-sun twin exoplanets at the image plane of a 10-m aperture. In table 1, we present a calculation of the angle in mas of a terrestrial exoplanet twin as a function of range from the earth in units of parsecs. Note that the earth-twin terrestrial exoplanets are located at angles between 50 and 10 milli-arc-seconds (mas).

Distance	Angle	Aperture
(pc)	(mas)	(m)
20	50	8.1
40	25	16.3
60	16.7	24.4
80	12.5	32.6
100	10.0	40.7

Table 1 Image plane location in milli-arc-seconds (mas) of earth-twin exoplanets as a function of distance or range from the earth in units of parsecs. Column 1 distance in parsecs, column 2 angular separation in mas between the parent star and the earth twin, and column 3 is the telescope aperture in m required to place the terrestrial exoplanet at the 3rd Airy diffraction ring of a 10-m aperture at 500-nm wavelength.

We next calculate the image plane location of the diffraction grating images of the parent star. We use the well-known diffraction grating equation and write:

$$n\lambda = 2d\sin\theta$$

Where n is the diffraction order, λ is the wavelength of light, d is the period of the grating (w/2 in this case) and θ is the angle of diffracted star image as it appears at the image plane for order n. Using this equation, we calculate the entries in table 2, below.

2d in m	Order n=1	450=>550 nm
Hex F to F in meters	Center mas	Dispersion mas
1	103	± 10.3
2	52	± 5.2
3	34	± 3.4

Table 2 image plane radius, in milliarcseconds (mas) from the central star at 500-nm for the diffraction order 1 and the radii of the resulting diffraction order n=1 grating spectrum from 450 to 550 nm wavelength for 1 , 2 and 3 meter "across the flats" hexagonal segments.

If we compare the angular location of the diffracted star (Table 2) with the location of candidate terrestrial exoplanets (Table 1) we see that diffraction and its resulting dispersion from the ensemble of hex segments cause the exoplanets to be masked.

For large aperture telescopes, we discovered a pinwheel segmented aperture topology that minimizes this diffraction-caused "noise" structure at the image-plane[9,10]. This topology and its performance are compared to that for a hexagonally segmented aperture in Figure 4, below.

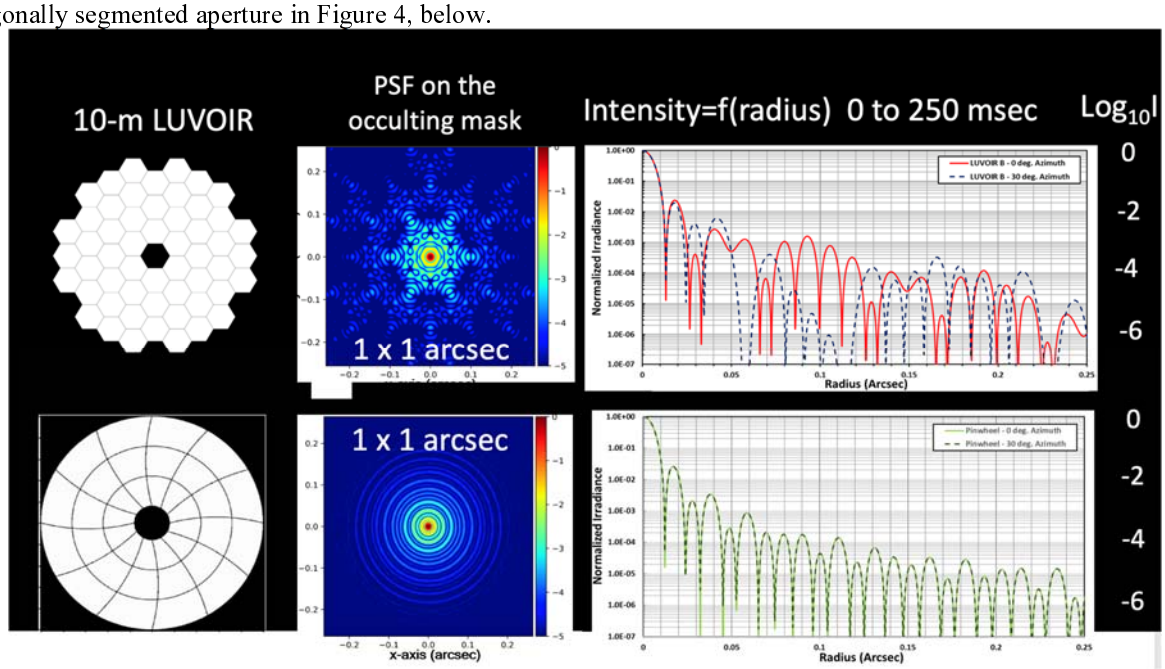

Figure 4. Monochromatic diffraction patterns for a modified LUVOIR-B aperture stretched from 8-m to 10-m diameter with 5-mm segment gaps is compared to a 10-m diameter pinwheel aperture with 5-mm segment gaps. Top row L to R: modified LUVOIR-B aperture map, log $_{10}$ stretch of the PSF and a plot of the normalized irradiance as a function of radius for 0^0 (red) and 30^0 (blue dots) azimuth angle. Bottom row L to R: pinwheel aperture map, log $_{10}$ stretch of the PSF and a plot of the normalized irradiance as a function of radius for 0^0 (green) and 30^0 (grey dots) azimuth angle. The center plots on a blue background show the expected system point spread function that falls onto the coronagraph occulting mask. The PSF structure shown at top-center indicates that many false-positive identification of exoplanets may occur and exoplanets would be masked if a hex segmented aperture is used.

The axially-symmetric pinwheel-aperture, for an on-axis "Cassegrain" telescope configuration is shown in the lower left of Fig 4. The Cassegrain secondary is suspended above the primary and held centered by curved vane structures. The vane structures are curved to match the pinwheel curvatures. The match is made by rotating or clocking the vanes to shadow the segment gaps. This aperture will be less expensive to fabricate, assemble, test and align than is the axially-symmetric hexagonal-segmented aperture because of the decreased diversity within the opto-mechanical mirror assembly. This primary aperture mirror requires building one curved and tapered wedge which has 3 optical prescriptions on each of three curved sided segments and then duplicating that wedge 12 times for the remainder of the aperture. An anticipated technical issue is the sharp angles on the surface of each segment. However, recent technical developments in magnetorheological polishing[11] of mirror surfaces indicate that the mirror substrate will hold an optical figure of 0.05 wave or better to the edge.

In addition to the obvious design, fabrication, test and alignment advantages of the pinwheel aperture there is a spacecraft system operational gain since the space-craft does not need to be bore-sight rolled to various field azimuth angles to accommodate the non-rotationally symmetric image plane mask introduced across the field by diffraction from the hexagonal segments. Almost twice as many terrestrial exoplanets can be characterized using the pinwheel aperture telescope/coronagraph system during the mission lifetime as can be characterized using an aperture tessellated with hexagonal segments.

Future work on the pinwheel aperture concept includes the design of a Lyot coronagraph for the PSF shown in Figure 4, lower center; with a quantitative assessment of the achievable contrast. This will be followed by an assessment of sensitivity of that contrast to polarization aberrations and mechanical dynamic deformations of the pinwheel aperture using software models and hardware testbeds.

One design approach that may eliminate the need for wide (~5-mm) gaps between segments is in-space assembly of the large aperture[12,13]. Such an approach should be actively considered.

Technology has been created by others to control the shape of the PSF by applying absorption masks to cover the gaps around the edges of each individual hex-segment shown in Fig 4, upper left.[14] The purpose is to remove the deleterious diffraction effects of hex segmented apertures. This additional absorption reduces the system transmittance and increases the complexity of the system leaving many questions. These include: stability of the mechanical alignment of the apodizer, the image plane mask, and optical dispersion introduced by the absorption.

7. INSTRUMENT/TELESCOPE POLARIZATION

In classical, non-diffraction limited imaging applications the polarizing properties of an imaging system are not noticeable. However, in complex very high-performance diffraction limited optical systems such as Lyot coronagraphs for space-based imaging of exoplanets, polarization is a major factor[15,16,17], particularly in terrestrial exoplanet imaging systems that require contrasts $<10^{-10}$. As the optical wavefront passes from object space through the telescope and reflects on through those optics before the coronagraph mask, the surface of the wavefront becomes partially polarized.[18] Different portions of the wavefront are polarized differently. This creates a distorted electric field (phase and amplitude) at the phase mask shown in Fig 1. To create a "perfect" coronagraph this electric field incident on the mask must match the electric field manipulating properties of the filter shown at the image plane in Figure 1.

Selecting the correct opto-mechanical layout during the geometric ray-trace design phase of the instrument corrects for Fresnel polarization aberrations that arises from non-normal incidence.[19] However, polarization changes across the surface of a wavefront caused by metal thin film anisotropies cannot be minimized or corrected using mechanical tip and tilt of mirror surfaces to correct polarization changes across the wavefront surface.[15]

Large aperture primary telescope mirrors require a high-reflecting metal thin film coating to reflect the broad wavelength band thermal radiation from the star-exoplanet system. As a result of the deposition processes in use today, these thin films are electronically anisotropic. Image quality degradation from polarization reflectivity changes across the surface of the primary is significant for coronagraphy.

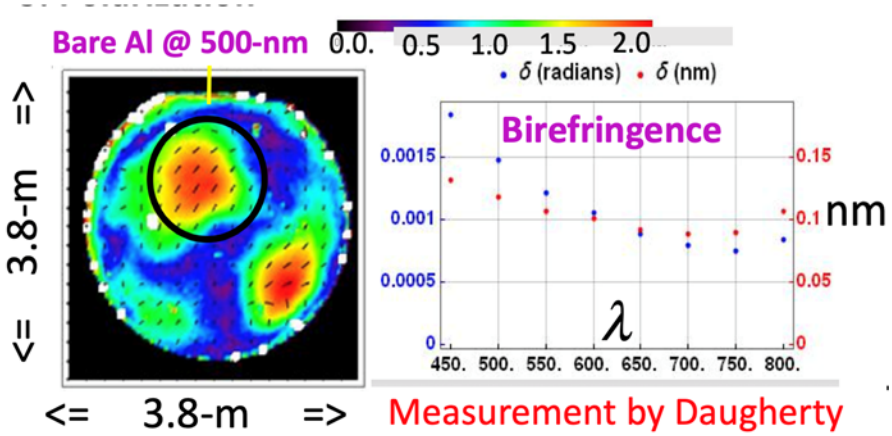

Figure 4. Spatially dependent complex polarization reflectivity for an aluminized 3.8-m test sphere at the University of Arizona Mirror Lab. The mirror was coated using the same processes as those used for the 4-meter diameter Mayall telescope on Kitt Peak. Measurements were made and interpreted by Dr. Daugherty from the center of curvature of the 3.8-m mirror[20]. The circle at the left shows a map of the form birefringence, or polarization phase error across the aperture. Retardance scale is shown in color across the top. The red patch is 2 mrad retarded referenced to the dark blue regions and the green region is retarded by 1 mrad. The graph on the right shows the birefringence in units of radians (scale on the left) and in nanometers (scale on the right) as a function of wavelength measured from 450 to 800 nm measured over the region shown in the black circle within the map on the left.

Current NASA test beds use small laboratory apertures to emulate the performance of large area primary mirrors in the 1 to 4-meter class. The laboratory mirrors do not exceed 10 to 15-cm diameter. Coating processes for these mirrors are very different than those that are needed on large aperture robust mirrors for space telescopes. Contrast measurements made using laboratory mirrors will be better than the system contrast achievable with large-aperture space qualified mirrors.

The 4-meter HabEx optical system was polarization ray-traced using the POLARIS-M ray-trace code and published.[15]

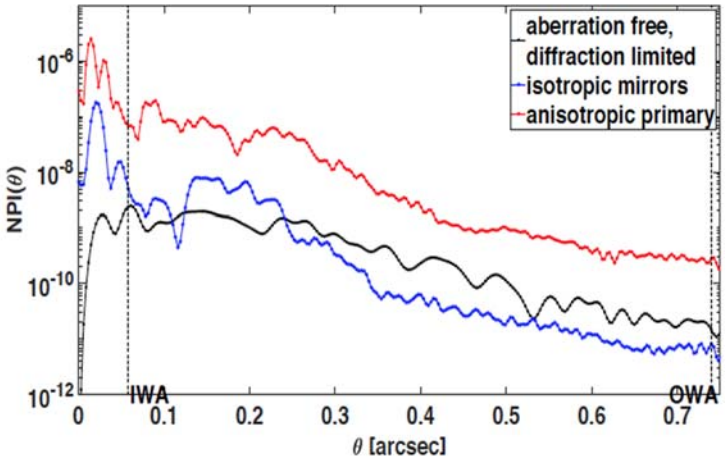

Figure 5 Normalized polychromatic irradiance (NPI), a measure of contrast, as a function of field angle at the detector plane using a vector cortex 6 mask in the 4-m aperture HabEx optical system is shown for slices in the horizontal (y=0) direction (a) and the vertical (x=0) direction (b) for the aberration-free case (black lines), the aberration case for isotropic mirrors (blue) and the aberration

case where the primary mirror has the birefringence map shown (red). Wavelength is centered at 500 nm with bandwidth 450 to 550 nm. This is the "blue channel" of the HabEx coronagraph instrument parameters described by Martin, et. al.[21] Field angles are from 0 to 0.75 arc second. Inner (58 mas) and outer (740 mas) working angles are shown. From reference 11.

Suggested processes to "anneal" the form birefringence to make uniform the form birefringence across the aperture include ion assisted deposition (IAD) techniques. However great care must be taken since IAD processes are known to increase mirror surface scatter, which is bad for terrestrial exoplanet characterization. Atomic layer deposition (ALD) technology may produce a surface with form birefringence. Neither of these deposition processes have been scaled to the >1-meter class surface areas that have a requirement on form birefringence.

8. SCATTERED LIGHT FROM MIRROR SURFACES

The surface of each thin film reflection and transmissive optical window and color filter within the telescope/instrument telescope scatters light to create unwanted background signal at the image plane.[22] If large enough, this background signal will mask the presence of terrestrial exoplanets. The magnitude of this background signal in astronomical systems is different than that for laser systems.

Dielectric coated mirrors designed for use over narrow wavelength bandpasses in high gain laser cavities come closest to having minimum scatter losses. However, this technology cannot be used in astronomical telescopes because astronomers need to have their large apertures coated with broadband highly reflective coatings such as metal aluminum and silver. The opto-electronic properties of metals exhibit more surface scatter than pure dielectrics.

Light from the very bright central star will be scattered into a narrow specular angle by the mirror surfaces to surround the PSF with an incoherent halo of light. This scattered light adds unwanted light incoherently to the telescope PSF to reduce the system contrast capability. This addition of light to the PSF is not controlled by adaptive optics, which change geometrical optical path lengths and not surface scatter. Current technology cannot accurately predict the amount of light forward scattered, sometimes called narrow angle scatter or angle resolved scatter (ARS) into the specular beam that forms the PSF.[23] These sources of scattered light have the potential to reduce instrument contrast and result in exoplanet spectra being seriously polluted with starlight.

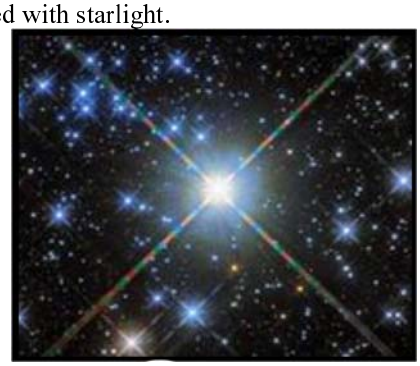

Figure 6. Image in color of an unknown bright star recorded with HST showing what appears to be a blue halo of scattered light around the star.

Assuming the telescope has no significant geometric or polarization aberrations, the optical system point spread function (PSF) is the incoherent linear superposition of two wavelength dependent PSF's, one from the Airy diffraction pattern and the other from the angle-resolved or narrow angle scatter. A portion of the near-specular scattered light manifests its appearance as white-light speckle[24,25]. The intensity and the halo size of the angle resolved scattering apparent within the small FOV of the star will depend on the wavelength,[26] which may account for the blue halo that appears around the color-image of the star in Fig 6.

9. FUTURE WORK

- Maximize transmittance
  - In both HabEx and LUVOIR, the image-plane field-point pick-off is off axis and additional mirror surfaces are needed to correct the geometric wavefront before the coronagraph. These additional surfaces result

increased absorption and surface scatter. Innovative application of new design principles (e.g. free-form optics) are needed to reduce the number of optical elements.

- Scalar diffraction
  - We have shown in this and earlier papers the compelling advantages of segmenting the primary in a pinwheel pattern, rather than regular hexagons for imaging purposes. However, it remains to be demonstrated quantitatively that the pinwheel aperture is advantageous for coronagraphy and to investigate its sensitivity to dynamic wavefront errors.
- Polarization aberrations
  - We have shown that large aperture primary mirror coatings used by astronomers exhibit form birefringence at levels ranging from 0.7 to 2 nm across the bandwidth between 400 and 800 nm. Polarization reflectivity varies significantly across the surface. The coating on the large aperture contributes to a decrease in contrast between 10 and 100 times.
  - An investigation into the material-science of coating highly reflecting large-area surfaces is needed to gain confidence that we can mitigate these effects.
- Small angle specular scattered light
  - No optical system has ever had a requirement to minimize small-angle specular-mirror scattered light. Investigations are needed into the source of small-angle specular-scattered light from both small and large area mirror surfaces.

10. ACKNOWLEDGEMENTS

This work was funded in part by NASA research grant NNX 17AB29G to James Breckinridge, PI, at the James C. Wyant College of Optical Sciences, University of Arizona, Tucson AZ. Additional support provided by: Caltech, and Photon Engineering, Tucson, AZ.

11. REFERENCES

[1] Breckinridge, J. B. [Basic Optics for the Astronomical Sciences] SPIE Press 423-page book ISBN 978-0-8194-8366-9 (2012)

[2] Breckinridge, J. B. , T. G. Kuper and R. V. Shack "Space Telescope Low-Scattered-Light camera: a model", Optical Engineering **23**, 816-820. (1984). Originally published 1982 as SPIE Proc 331: conference on Instrumentation in Astronomy IV, Tucson AZ. 9 March 1982.

[3] Lyot, Bernard "Photographie de la couronne solaire en dehors des eclipses" CR Acad. Sci. Paris **193**, 1169 p 48 (1931)

[4] Bolcar, M., K. N. Balasubramanian, M. Clampin, J. Croocke, L. Feinberg, M. Postman, et. al. "Technology development for advanced large aperture space telescope (ATLAST) as a Candidate LUVOIR system", (2015)

[5] Lillie, C. F. and J. B. Breckinridge "Prime focus architectures for large space telescopes: reduce surfaces to save cost", Proc SPIE 9904 – 4K (2016)

[6] Chipman, R. A. and Wai Sze T. Lam and James Breckinridge "Polarization Aberration in Astronomical Telescopes", Proc. SPIE 9613-16 (2015)

[7] Bennett, J. M. , J. M. Elson and J. P. Rahn "Angle resolved Scattering: comparison of Theory and experiment in Thin Film Technologies", J. R. Jacobsson, ed. Proc SPIE 401, 234-246 (1983)

[8] Kaya, I. K. P. Thompson, J. P. Rolland "Comparative assessment of freeform polynomials as optical surface descriptions". Optics Express 20, 22683-22691, (2012)

[9] Harvey, James E., James B. Breckinridge, Ryan G Irvin, Richard N. Pfisterer, (2018) "Novel Designs for minimizing diffraction effects in large segmented mirror telescopes", SPIE 10745 -0L

[10] Breckinridge, James B. , James Harvey, Karleton Crabtree, et. al. "ExoPlanet telescope diffracted light minimized: the pinwheel pupil solution", SPIE Proc 10698-1P (2018)

[11] Chunlin Miao, Shai Shafrir, John Lambropoulos, Joni Mici, et. al. "Shear stress in magnetorheological finishing for glasses", Applied Optics 48, 2585-2595, (2009)

[12] Lillie, C. F. , H. A. MacEwen, R. S. Polidan and J. B. Breckinridge "A 4-m evolvable space telescope configured for NASA's HabEx Mission: the initial stage of LUVOIR", Proc. SPIE 103980R (2017)
[13] Polidan, R. S., Breckinridge, J. B., Lillie, C. F., MacEwen, H. A., Flannery, M. R., and Dailey, D. R., "Innovative telescope architectures for future large space observatories", JATIS 2(4), 041211, (2016)
[14] N'Diaye, M., R.Soummer, L Pueyo, A. Carollitti, C. Stark and M. Perrin, "Apodized pupil Lyot coronagraphs for arbitrary apertures V. hybrid shaped pupil designs for imaging earth-like planets with future space observatories". ApJ 818:163 (2016)
[15] Breckinridge, James B. , Wai Sze T. Lam and Russell A. Chipman (2015) [Polarization Aberrations in Astronomical Telescopes: The Point Spread Function], Publications of the Astronomical Society of the Pacific, **127**:445-468
[16] Breckinridge, J. B. , M. Kupinski, J. Davis, B. Daugherty and R. A. Chipman "Terrestrial exoplanet coronagraph image quality polarization aberrations in Habex", SPIE Proceedings 10698-1D (2018)
[17] Davis, Jeffrey, Meredith K. Kupinski, Russell A. Chipman, James B. Breckinridge and Brian Daugherty "HabEx Polarization Ray Trace and Aberration Analysis" SPIE Proceedings 10698-3H (2018)
[18] Chipman, Russell A. , Wai Sze Tiffany Lam, and Garam Young [Polarized Light and Optical Systems] 979 page textbook (2019)
[19] Lam, Wai Sze Tiffany & Russell Chipman, "Balancing polarization aberrations in crossed fold mirrors", Applied Optics **54** 3236-3245, (2015)
[20] Daugherty, Brian [Examples of optical design where polarization was a primary requirement], PhD dissertation in Optical Sciences, James C. Wyant College of Optical Sciences, University of Arizona, Tucson. (2019)
[21] Martin, S., M. Rud, P. Scowen, D. Stern, J. Nissen and J. Krist "Habex Space Telescope Optical System" SPIE Proc TBD, Table 7. (2017) SPIE Proc 1039805.
[22] Stover, John C. [Optical Scattering: measurement and analysis] SPIE optical engineering press 321 page book. (1995)
[23] Harvey, James E., [Understanding Surface Scatter Phenomena: a linear systems formulation], SPIE Press - 234 pages ISBN 1510627871 (2019)
[24] Goodman, J. W. "Some properties of speckle from smooth objects" Optical Engineering 49 068001-1 to -9 (2010)
[25] Goodman, J. W. [Statistical Optics], Wiley series in pure and applied optics 516 page book (2015)
[26] Bennett, J. M. and L. Mattson (1999) "Angle resolved scattering, Introduction to Surface Roughness and Scattering 2nd ed." Optical Society of America Press, Washington DC. page 66 to 68.